

1961

Columns under combined bending and thrust,
Proc. ASCE, 85 (EM2), p. 1, (1959), (also ASCE
Trans. Vol. 126, (1961), Reprint No. 136 (61-22))

T. V. Galambos

R. L. Ketter

Follow this and additional works at: <http://preserve.lehigh.edu/engr-civil-environmental-fritz-lab-reports>

Recommended Citation

Galambos, T. V. and Ketter, R. L., "Columns under combined bending and thrust, Proc. ASCE, 85 (EM2), p. 1, (1959), (also ASCE Trans. Vol. 126, (1961), Reprint No. 136 (61-22))" (1961). *Fritz Laboratory Reports*. Paper 29.
<http://preserve.lehigh.edu/engr-civil-environmental-fritz-lab-reports/29>

This Technical Report is brought to you for free and open access by the Civil and Environmental Engineering at Lehigh Preserve. It has been accepted for inclusion in Fritz Laboratory Reports by an authorized administrator of Lehigh Preserve. For more information, please contact preserve@lehigh.edu.

RESEARCH INSTITUTE OF THE UNIVERSITY OF CALIFORNIA



Welded Continuous Frames and Their Components
PROGRESS REPORT—26

COLUMNS UNDER COMBINED BENDING and THRUST

by
Theodore V. Galambos
Robert L. Ketter

APRIL 1958

620.5
L527F
N0.205A.21

Fritz Engineering Laboratory Report No.205A.21

Welded Continuous Frames and Their Components

Progress Report No. 26

COLUMNS UNDER COMBINED BENDING AND THRUST

by

Theodore V. Galambos
Robert L. Ketter

This work has been carried out as a part of an investigation sponsored jointly by the Welding Research Council and the Department of the Navy with funds furnished by the following:

American Institute of Steel Construction
American Iron and Steel Institute
Institute of Research, Lehigh University
Column Research Council (Advisory)
Office of Naval Research (Contract Nonr 610(03))
Bureau of Ships
Bureau of Yards and Docks

Reproduction of this report in whole or in part is permitted for any purpose of the United States Government.

Fritz Engineering Laboratory
Department of Civil Engineering
Lehigh University
Bethlehem, Pennsylvania

April, 1958

Fritz Engineering Laboratory Report No. 205A.21

SYNOPSIS

Interaction curves relating the axial thrust, applied end bending moment and slenderness ratio are developed for the ultimate carrying capacity of pin-ended, wide-flange beam-columns. It is assumed that failure is due to excessive bending in the plane of the applied moments which is further considered to be the plane of the web. The two conditions of loading that are investigated are 1) equal end moments applied such that the resulting deformation is one of single curvature, and 2) end moment applied only at one extremity of the member. The influence of an assumed symmetrical residual stress pattern is considered in the calculations and curves are presented for slenderness ratios up to and including $L/r = 120$. For ease of future computations, the interaction curves are fitted into approximate equations. Comparisons are made with various column test results.

TABLE OF CONTENTS

	<u>Page</u>
SYNOPSIS	
I. INTRODUCTION	1
II. DETERMINATION OF INTERACTION CURVES	4
III. APPROXIMATE INTERACTION EQUATIONS	9
1. Condition "c" Loading	9
2. Condition "d" Loading	10
3. "C.R.C. Interaction Equation"	11
4. Axially Loaded Column	12
IV. COMPARISON WITH TEST RESULTS	12
V. DISCUSSION AND SUMMARY	18
VI. ACKNOWLEDGEMENTS	19
VII. REFERENCES	20
VIII. NOMENCLATURE	22
IX. APPENDIX	
1. Tables	
2. Figures	

I. INTRODUCTION

When designing (or analyzing) a structure by the simple plastic theory, it is assumed that the member in question will deliver the fully plastic moment value, M_p , noted in the calculations. This, however, will not necessarily be the case if the member is subjected to an axial thrust in addition to bending moments^{(1)*}. To attain the desired moment value, it is necessary to supply a member having a greater M_p value than the one needed for pure bending; i.e., one that will develop the required end moment in the presence of the imposed axial thrust.

The problem that will be considered in this paper is the determination of the maximum amount of end bending moment that a member can sustain when it is also subjected to a given axial thrust. Two loading cases will be investigated:

- 1) axial thrust plus equal end moments applied at both ends of the member such that it deforms in single curvature, and
- 2) axial thrust plus moment applied only at one end of the member.

These conditions are shown diagrammatically as loading conditions "c" and "d" in Fig. 1. In both cases it is assumed that the plane of the applied moments is that of the web of the section and that failure is due to excessive bending in this same plane.

* Numbers in parentheses refer to the list of references at the end of the report.

The stress-strain properties of the material are pre-supposed to be ideally elastic-plastic; i.e., there is initially a linear range wherein $\sigma = E\epsilon$ which is followed by a constant stress level $\sigma = \sigma_y$ for strains greater than ϵ_y^* . (This type of behavior is typical of mild structural (ASTM A7) steel if strain-hardening is neglected.) There is, however, assumed to be a symmetrical residual stress pattern present in the member prior to the application of any external loads. The presumed pattern (see Fig. 2) is consistent with measured residual stresses in wide-flange column type sections due to cooling of the section during and after rolling. (2), (3)

As shown in Ref. 2, if the material is homogeneous and isotropic and if bending strains are assumed to be proportional to the distance from the neutral axis, then the thrust-moment-curvature relationship for the 8WF31 section will be that given in Fig. 3. In this figure two conditions are illustrated. The solid lines are for the cases where residual stresses are neglected. The solutions which include the influence of the residual stress pattern shown in Fig. 2 are given by the dashed lines in Fig. 3.

Since the basic approach that will be used in solving the problem considered in this paper is one of numerical integration, and since this integration will proceed from a knowledge of the curvature values of Fig. 3, which as was stated above were computed for the 8WF31 section, the resulting interaction curves

* The nomenclature is given in Section IX.

will in the strictest sense apply only to the 8WF31 section. It should be noted, however, that this section has one of the more severe thrust-moment-curvature relationships of the column sections rolled. Using the interaction curves for other shapes should therefore result in a conservative or at least equal prediction of strength for the member in question.

For ease of presentation and generalization, load and section property parameters have been non-dimensionalized wherever possible. It was necessary, however, to consider a fixed value of Young's Modulus at $E = 30,000,000$ psi. Since specifications require a minimum yield stress of $\sigma_y = 33,000$ psi for A7 steels, this value was also used in the calculations as the base yield stress.

While the nondimensional loading parameters P/P_y and M/M_p implicitly take into account the influence of σ_y , the slenderness ratio must be modified for a material having a yield stress level other than 33,000 psi. Using as a base for this correction the slenderness ratio for which the stress corresponding to the "Euler load" equals the yield stress value, the adjusted slenderness ratio will be according to the following equation:

$$\left(\frac{L}{r}\right)_{\text{Adj.}} = \left(\frac{L}{r}\right) \sqrt{\frac{\sigma_y}{33,000}} \dots \dots \dots (1)$$

where σ_y = yield point stress in lbs. per sq. inch. When comparing test results with strength predictions, the adjusted slenderness ratios of the test members are used.

II. DETERMINATION OF INTERACTION CURVES

As was pointed out in the preceding section, the approach that will be used in the solution of the problem in question will be one of numerical integration⁽⁴⁾. This will proceed from an assumed deflection configuration and will take into account the non-linearity between moment and curvature as strains exceed the initial yield strain.

Since deflections must be assumed, it is desirable to know the equation of the column centerline at initiation of yielding for each of the conditions of loading. These can be determined from a consideration of the equations on page 12 of Ref. 5. In terms of the parameters used in this report, the equations are as follows:

- a) Moments applied at both ends of the member
(condition "c")

$$y = \frac{S}{A} \left[\frac{M_o/M_y}{P/P_y} \right] \left[\frac{\sin kx}{\sin kL} + \cos kx - (\cot kL)(\sin kx) - 1 \right] \dots (2)$$

- b) Moment applied only at one end of the member
(condition "d")

$$y = \frac{S}{A} \left[\frac{M_o/M_y}{P/P_y} \right] \left[\frac{\sin kx}{\sin kL} - \frac{x}{L} \right] \dots \dots \dots (3)$$

In these equations

S = section modulus,

A = cross-sectional area,

x = distance along member as shown in Fig. 1

y = lateral deflection of the column centerline in the plane of bending, and

$$k = \sqrt{P/EI}$$

For the assumed values of $E = 30,000,000$ psi and

$$\sigma_y = 33,000 \text{ psi}$$

$$kL = 0.003317 \left(\frac{L}{r}\right) \sqrt{\frac{P}{P_y}}$$

and

$$kx = 0.003317 \left(\frac{x}{L}\right) \left(\frac{L}{r}\right) \sqrt{\frac{P}{P_y}}$$

. (4)

From Equations (2) and (3) it can be seen that for the conditions of constant axial thrust and elastic behavior there is a linear relationship between the applied end moment, M_0 , and the resulting deformation. The maximum value of M_0 for which this situation holds is referred to as the initial yield value and the solution to this problem has been presented in Ref. 6 and elsewhere. For greater values of applied end moment yielding will occur at the most highly strained sections along the member. In these regions the member becomes relatively weaker to further increases in loading. This can be seen from the moment-curvature diagrams of Fig. (3). The load-deformation relationship of the member as a whole will also indicate this decrease in stiffness but in the early stages at a less pronounced rate. This follows from the fact that the total deformation is the integrated effect of all of the curvature values along the length of the member.

To be able to determine the maximum carrying capacity of a given member, it is essential that the load-deformation relationship of that particular member be defined. But since, as was noted earlier, a numerical integration procedure is to be used, it is first of all necessary to assume deflection values along the member and successively correct these assumptions based on the corresponding integrated curvature values. The process must be repeated until the desired accuracy of the deflected shape is obtained. For any one member and axial thrust ratio, then, the definition of the load-deformation relationship above the elastic limit, and thereby the definition of the critical loading, may require the consideration of four or five end moment values which in turn may require three or four numerical integrations each.

In addition, for a given slenderness ratio, it is necessary to determine the critical value of the end moment for various values of the axial thrust. This would make it possible to define the relationship between axial thrust and end moment for this one particular slenderness value; i.e., to define the interaction curve for this given slenderness ratio. In general 0.2 P/P_y intervals were used in the computations on which the interaction curves of this report are based. For a better definition of the relationship at higher values of thrust, however, a closer spacing of values of P/P_y was used. Slenderness ratios ranging from 0 to 120 were considered in intervals of 20.

In outline form, then, the steps that were used in determining each of the interaction curves presented in this report are as follows:

GIVEN: loading condition, slenderness ratio and constant axial thrust value for the 8WF31 Section used as a standard.

1. Assume an end moment, M_0 , greater than the initial yield value;
2. Assume a possible deflection configuration; (as a first approximation, the elastic limit deflections defined by Equations (2) and (3) could be used.)
3. Knowing the moment values at eight equally spaced stations along the length of the member ($M_x = M_{0x} + Py$), numerically integrate curvature values obtained from Fig. 3 (an enlarged version of this figure was used). (See Fig. 5);
4. Correct the assumed deflections based on the values obtained from this numerical integration and repeat step (3);
5. Repeat step (4) until the desired accuracy is obtained (± 0.001 inch was used in this report);
6. Determine the end rotation for the final deflection values of step (5)*

* If it is assumed that the deflection curve of the member within the three end segments can be represented by a parabola, then the end slope can be expressed in terms of the known deflection as

$$\theta_0 = \frac{4\delta_1 - \delta_2}{2\lambda}$$

where

- δ_1 = deflection at first station away from the applied moment end of the member,
 δ_2 = deflection at the second station away from the applied moment end of the member, and
 λ = grid spacing (assumed to be $L/8$ for the cases

7. Assume greater values of the end moment, M_0 , and repeat the same process as outlined above;*
8. Plot the various values of M_0 versus θ_0 from step (7) and determine the maximum value of M_0 from the resulting curve. (See Fig. 4).

This gives one particular point on one particular interaction curve. As was pointed out above, it is necessary to determine many such points to be able to define the desired range of the interaction curves.

Dividing the (M_0/M_y) critical values obtained from the numerically determined M_0 versus θ_0 curves by the shape-factor, the interaction curves of P/P_y versus M_0/M_p versus L/r shown in Figs. 6 and 7 were obtained. Fig. 6 is for the case of moments applied at both ends of the member (condition "c") and Fig. 7 is for the case of moment applied at one end (condition "d"). Only the interaction curves incorporating the influence of residual stress have been included in this report. However, interaction curves neglecting these stresses as well as the corresponding initial yield interaction curves are shown in Ref. 7. Also given therein is a more detailed explanation of the derivation of the curves shown in Figs. 6 and 7. To give an indication of the influence of residual stress on the carrying capacity of members of the type considered herein, Fig. 8 gives comparable interaction curves for an $L/r = 80$.

* If an M_0 greater than or equal to $M_0(\text{critical})$ is assumed, the numerical integration process yields divergent results.

To make the curves more useful when eccentricity ratios (ec/r^2) are given instead of end moments, values of ec/r^2 are also shown on the interaction curve figures.

III. APPROXIMATE EQUATIONS

To avoid interpolating from the diagrams of Figs. 6 and 7, approximate interaction equations were developed by fitting the curves into cubic and quadratic equations. All of the limitations of the original curves are therefore present in these approximations. In general, the range of application was chosen as $0 \leq L/r \leq 120$ and $0 \leq P/P_y \leq 0.6$. It was considered that these covered the major range of practical applications.

- 1) Pin-ended column subjected to axial thrust plus two equal end-moments applied such that the resulting deformation is that of single curvature (condition "c"):

Assuming an equation of the form

$$\frac{M_o}{M_p} = 1 - K \left(\frac{P}{P_y}\right) - J \left(\frac{P}{P_y}\right)^2 \dots \dots \dots (5)$$

where K and J are assumed to be functions only of the slenderness ratio, the coefficients of the axial load terms of the equation were found to be

and

$$\left. \begin{aligned} K &= 0.420 + \frac{(L/r)}{70} - \frac{(L/r)^2}{29,000} + \frac{(L/r)^3}{1,160,000} \\ J &= 0.770 - \frac{(L/r)}{60} + \frac{(L/r)^2}{8,700} - \frac{(L/r)^3}{606,000} \end{aligned} \right\} \dots \dots \dots (6)$$

The agreement between these expressions and the comparable relationship from Fig. 6 is as shown in Fig. 9. The direct correlation between the approximate equations and the interaction curves of Fig. 6 is given in Fig. 10.

2) Pin-ended column subjected to axial thrust plus an end-moment applied only at one end of the member (condition "d"):

Assuming an equation of the form

$$\frac{M_o}{M_p} = B - G \left(\frac{P}{P_y} \right) \dots \dots \dots (7)$$

where (as in case 1) B and G are assumed to be functions only of the slenderness ratio, the coefficients are found to be

$$G = + 1.110 + \frac{(L/r)}{190} - \frac{(L/r)^2}{9,000} + \frac{(L/r)^3}{720,000}$$

and

$$B = 1.133 + \frac{(L/r)}{3080} + \frac{(L/r)^2}{185,000}$$

} \dots (8)

It should be noted that when Equation (7) predicts a value of M_o/M_p greater than 1.00 (that is, for small values of P/P_y), $M_o/M_p = 1.00$ should be used.

The agreement between the approximate interaction Equation (7) and the relationships determined numerically (Fig. 7) is shown in Fig. 11.

Table 1 is a tabulation of the interaction equation constants B, G, J and K for L/r values from 0 to 120 varying in increments of 5.

3) "C.R.C. Interaction Equation"

Recently, attention has been focused on the application of the so-called "C.R.C. interaction equation" to the first ("c") condition of loading⁽⁸⁾.

$$\frac{P}{P'} + \frac{M_o/M'}{1-P/P_e} = 1 \dots\dots\dots (9)$$

where

- P' = maximum axial thrust that the member will sustain when subjected to pure axial thrust;
- M' = maximum end moment that the member will sustain when subjected to pure bending; and
- P_e = Euler buckling load for the axially loaded member.

Since it was assumed in the derivation of the interaction curves presented earlier in this report that the member did not fail by lateral instability, M' of Equation (9) should be taken equal to M_p. Equation (9) then becomes

$$\frac{M_o}{M_p} = 1 - K' \left(\frac{P}{P_y}\right) - J' \left(\frac{P}{P_y}\right)^2$$

where

$$\left. \begin{aligned} K' &= \zeta \left(\frac{L}{r}\right)^2 + \frac{P_y}{P'} \\ J' &= - \left(\frac{P_y}{P'}\right) \left(\frac{L}{r}\right)^2 \zeta \end{aligned} \right\} \dots\dots\dots (10)$$

and

$$\zeta = \frac{\sigma_y}{\pi^2 E}$$

In Fig. 9, the expressions for K' and J' (determined from Equations 10 using for (P'/P_y) the end points of Fig. 6 or 7) are compared with the values determined by numerical integration.

4) Axially Loaded Columns

Approximating that portion of the relationship between axial thrust and slenderness ratio that occurs below the Euler curve (that is, $0 \leq L/r \leq 112$), the following expression may be used

$$\frac{P}{P_y} = 1 - \frac{1}{645} \left(\frac{L}{r}\right) - \frac{1}{111,000} \left(\frac{L}{r}\right)^2 \dots \dots \dots (11)$$

Since this equation almost coincides with the numerically determined values shown in Figs. 6 and 7, a comparison has not been shown.

It is gratifying to note the close correspondence between Equation (11) of this paper and Equation (20) of Ref. 17 by Bijlaard, Fisher and Winter, since the latter expression was determined by an entirely different procedure.

IV. COMPARISON WITH TEST RESULTS

As an experimental check of the theoretical predictions of this report, existing test data are compared with the interaction curves of Figs. 6 and 7. The tests of the following experimental programs are used for comparison:

1. Cornell University, 1956 (Ref. 9)
2. Lehigh University, 1940 (Ref. 10)

3. University of Liege, 1956 (Refs. 11, 12)
4. University of Wisconsin, 1920's (Ref. 13)
5. Lehigh University, current series (Refs. 2, 6)

Graphs comparing the analytical predictions with experimental results are shown in Figs. 12, 13, 14, 15 and 16.

For a majority of the columns that have been tested and are listed herein, the members were subjected to eccentrically applied thrusts. In graphically comparing these test results with the strength predictions of this report slenderness values have been shown as the abscissa and (P/P_y) values as the ordinate (i.e., in the form of column curves for constant eccentricity ratios). The individual curves for each of the situations were obtained from Figs. 6 and 7 using the ec/r^2 values shown across the top and along the right hand side of the figure. It should be noted that since

$$\frac{ec}{r^2} = \left[\frac{M/M_p}{P/P_y} \right] \left[f \right]$$

and since the values of ec/r^2 given in Figs. 6 and 7 were obtained by using "f" of the 8WF31 shape (one of the lowest shape factors), the theoretical curves should be somewhat conservative for most of the sections tested.

CORNELL UNIVERSITY (Ref. 9)

These tests carried out by Mason, Fisher and Winter were on a cross-section which fully prevented lateral-torsional buckling and therefore conformed to the assumptions

of this report. Two "Z" sections were welded together in the form of a "hat" by intermittent welds. Bending was forced (by the use of knife-edges) about the minor axis of the total cross-section.

Figure (12) shows the comparison between the test results of Mason, Fisher and Winter and the theoretical predictions of Fig. 6. In general the correlation is quite good. The experimental results fall slightly above the predicted curves as would be expected since the shape factors of the sections tested ($f = 1.18, 1.25$ and 1.17) were greater than those of the 8WF31 section. Also, the residual stress distributions of the sections tested were not as severe as those that were assumed.

Table (2) gives a tabulation of the data from which the test points of Fig. 12 were plotted.

LEHIGH UNIVERSITY (Ref. 10)

A total of 93 tests were carried out by Johnston and Cheney in this series: 89 were made on 3I5.7 sections and 6 on 6WF20 sections. A summary of the test data is given in Table (3).

Columns were tested by both concentric and eccentric application of the axial load; however, the column tests under pure axial thrust cannot be compared with the predicted interaction curves. The end-condition of these test specimens were such that they fail by buckling about the weak axis.

In general, the tests were performed on columns which were essentially pin-ended with respect to bending in the strong direction and fixed-ended in the weak direction. This was accomplished by the use of knife-edges placed perpendicular to the web through which the load was applied. The loading conditions and support arrangements for the tests correspond to the condition "c" loading of this report (Fig. 6).

As noted in Table 3, the slenderness-ratios were adjusted to account for the yield stress of the material tested. The comparisons between predicted strengths and experimental results are shown in Fig. (13).

Johnston and Cheney report that the "columns loaded eccentrically to produce bending in the strong direction usually failed by plastic lateral torsional buckling" (a condition specifically excluded in this paper). It is interesting to note, however, that except for the tests which fall close to the case where failure would have been due to Euler buckling in the weak direction, the correlation achieved with the developed theory which neglects lateral-torsional behavior is reasonably good.

UNIVERSITY OF LIEGE (Ref. 11, 12)

Massonnet reports the results of 95 column tests. The tests were carried out on sections of DIE 10, DIE 20 and PN 22 profiles. Of these, the DIE profiles are geometrically similar to the American wide-flange shape, the shape being considered

in this report. Therefore, only the DIE profile tests will be used for comparison. Furthermore, only those tests which correspond to the condition "c" and "d" loading are listed.

The end conditions for Massonnet's test columns were essentially pin-ended in both directions since the end-fixtures consisted of almost frictionless, hydraulically seated steel hemispheres. For such end-conditions, the least possible restraint is provided against lateral torsional buckling.

Table 4 summarizes the applicable test data for the DIE profile tests. Figure (14) gives the comparison between the tests on members subjected to a condition "d" loading and the theoretical predictions shown by the dot-dash curves. As before, the slenderness ratio is adjusted for differences in yield stress level. In all cases the final failure was by lateral torsional buckling; in spite of this, most of the test points agree rather well with the theoretical relationship that neglects this type of failure. It is expected that further theoretical work taking this mode of failure into account will provide a better understanding of the problem and will result in a better correlation in the "transition range".

No comparison has been shown for the condition "c" tests of Ref. 12 (equal and opposite end moments). Due to the condition of loading and end restraints it would be expected that lateral-torsional instability would occur prior to the theoretical load predicted in this paper and this was

found to be the case. A solution to the problem of lateral-torsional buckling for this condition of loading which also takes into account the influence of residual stress has just been completed. In general, the correlation is quite good. A report on this latter work will soon be available.

UNIVERSITY OF WISCONSIN (Ref. 13)

The members tested in this investigation were 8H32 shapes, similar to the currently available 8WF31 section. The end-conditions were essentially pin-ended against strong axis bending and fixed in the weak direction. Of the five tests carried-out, the two which had an adjusted slenderness value greater than 50 failed by lateral-torsional buckling at a load slightly less than that predicted.

LEHIGH UNIVERSITY (Ref. 2, 6, 16)

Table (6) summarizes the results of the tests in this series that are applicable. Since the majority of the members were tested in a range where the interaction curves converge to a point (i.e., for low values of P/P_y) most of these have not been shown on graphs. For the pure axial load tests, however, Fig. 16 shows the correlation with predicted strength. An additional test by Huber⁽¹⁴⁾ (4WF13, $L/r=130$) has been included to extend the range of coverage.

V. DISCUSSION AND SUMMARY

For the conditions of end restraint and the loading conditions of Fig. 1, solutions to the problem of the determination of the maximum carrying capacity of wide flange shapes loading in the plane of the web have been presented. These solutions assume that the member in question will fail by excessive bending in the plane of the applied moment. Failure due to lateral-torsional or local buckling has not been considered. The resulting interaction curves (Figs. 6 and 7) do, however, include the influence of a typical cooling type residual stress pattern.

Approximate interaction equations, which cover the range most often encountered in practice, were developed to eliminate the need for interpolation (Equations 5 and 7).

Currently available test results were compared against the strength predictions of Figs. 6 and 7. The tests carried out by Mason, Fisher and Winter were the only ones that directly fulfill the assumptions of this report and the correlation was shown to be very good (Fig. 12). For the cases where the members tested were pin-ended in the strong direction and fixed in the weak, the curves give reasonably reliable results provided Euler buckling in the weak direction was not imminent (Figs. 13, 15 and 16). Where the members were pin-ended in both directions, lateral-torsional buckling was a major factor in determining strength (Fig. 14). The test

results corresponding to this situation (Massonnet) seem to indicate that for a condition "d" type of loading the overall behavior can still be approximated by the curves of Fig. (7) but with less accuracy than in the aforementioned cases (Fig. 14). Members loaded in a condition "c" manner, however, carry markedly less load than predicted.

Further work is currently underway to include the influence of lateral-torsional instability into the strength calculations and preliminary results of this study indicate that good correlation can be achieved when this type of failure is considered.

VI. ACKNOWLEDGEMENTS

This study was part of the general investigation "Welded Continuous Frames and Their Components" currently being carried-out at Fritz Engineering Laboratory, Lehigh University under the general direction of Lynn S. Beedle. The investigation is sponsored jointly by the Welding Research Council and the Department of the Navy with funds furnished by the American Iron and Steel Institute, American Institute of Steel Construction, Office of Naval Research, Bureau of Ships and Bureau of Yards and Docks.

William J. Eney is Director of Fritz Engineering Laboratory and Head of the Department of Civil Engineering.

VII. REFERENCES

1. Beedle, L.S., Thurlimann, B., and Ketter, R.L.,
"PLASTIC DESIGN IN STRUCTURAL STEEL-LECTURE NOTES",
AISC and Lehigh University, September 1955
2. Ketter, R.L., Kaminsky, E.L., and Beedle, L.S.,
"PLASTIC DEFORMATION OF WIDE-FLANGE BEAM COLUMNS",
Transactions of the ASCE, Vol. 120, 1955, p. 1028
3. Ketter, R.L.,
"THE INFLUENCE OF RESIDUAL STRESS ON THE STRENGTH OF
STRUCTURAL MEMBERS",
Proceedings of the 7th Technical Session of the
Column Research Council, May 1957
4. Newmark, N.M.,
"NUMERICAL PROCEDURES FOR COMPUTING DEFLECTIONS,
MOMENTS AND BUCKLING LOADS",
Transactions of the ASCE, Vol. 108, 1943, p. 1161
5. Timoshenko, S.,
"THEORY OF ELASTIC STABILITY",
McGraw-Hill Book Co., New York, 1939
6. Ketter, R.L., Beedle, L.S., and Johnston, B.G.,
"COLUMN STRENGTH UNDER COMBINED BENDING AND THRUST",
The Welding Journal 31(12), Research Supplement,
607-s to 662-s 1952
7. Galambos, T.V., and Ketter, R.L.,
"FURTHER STUDIES OF COLUMNS UNDER COMBINED BENDING
AND THRUST",
Fritz Engineering Laboratory Report No. 205A.19,
June 1957
8. A Report of Research Committee E of Column Research
Council
"SOME RECOMMENDATIONS RELATING TO DESIGN SPECIFICATIONS
FOR STEEL BEAMS AND MEMBERS SUBJECTED TO COMPRESSION
AND BENDING",
May 1954
9. Mason, R.E., Fisher, G.P., and Winter, G.,
"TESTS AND ANALYSIS OF ECCENTRICALLY LOADED COLUMNS",
Dept. of Structural Eng., School of Eng., Cornell Univ.,
Ithaca, New York April 1956
10. Johnston, B.G., and Cheney, L.,
"STEEL COLUMNS OF ROLLED WIDE FLANGE SECTION",
Progress Report No. 2, American Institute of Steel
Construction, November 1942

11. Massonnet, C., and Campus, F.,
"CORRESPONDENCE ON THE 'STAUCHION PROBLEM IN FRAME STRUCTURES DESIGNED ACCORDING TO ULTIMATE CARRYING CAPACITY' by Horne, M.R.",
Proc. Inst. of Civil Engrs. par III, Vol. 5,
p. 558-571 August 1956
12. Massonnet, C., and Campus, F.,
"RECHERCHES SUR LE FLAMBEMENT DE COLONNES EN ACIER A 37, A PROFIL EN DOUBLE TE, SOLLICITEES OBLIQUEMENT",
I.R.S.I.A. Bulletin No. 17, April 1956
13. "SECOND PROGRESS REPORT OF THE SPECIAL COMMITTEE ON STEEL COLUMNS"
Paper No. 1789, ASCE Transactions, Vol. 95, 1931
14. Huber, A.W.,
"THE INFLUENCE OF RESIDUAL STRESS ON THE INSTABILITY OF COLUMNS",
Lehigh University Dissertation, May 1956
15. Gozum, A.T., and Huber, A.W.,
"MATERIAL PROPERTIES, RESIDUAL STRESSES AND COLUMN STRENGTH",
Fritz Engineering Report No. 220A.14, May 1955
(Revised November 1955)
16. Beedle, L.S., Ready, J.A., and Johnston, B.G.,
"TESTS OF COLUMNS UNDER COMBINED THRUST AND MOMENT",
Proceeding, Society for Experimental Stress Analysis VIII, No. 1, 109 (1950)
17. Bijlaard, P.P., Fisher, G.D., Winter, G.,
"ECCENTRICALLY LOADED, END-RESTRAINED COLUMNS"
Transactions of the ASCE, Vol. 120, 1955 p. 1070

VIII. NOMENCLATURE

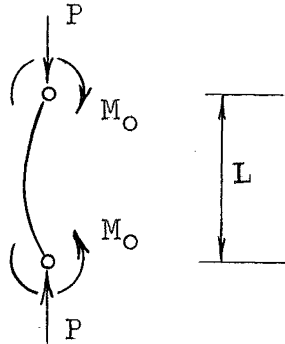
A	Area of cross-section (in ²)
B,G,J,K	Non-dimensional constants
E	Young's Modulus of Elasticity (E=30,000,000 psi for A7 steel)
I	Moment of Inertia (in ⁴)
L	Length of member (inches)
M	Bending Moment (inch-kips)
M ₀	Applied moment at the end of the member
M _p =Zσ _y	Fully plastic moment value under pure moment
M _y =Sσ _y	Initial yield moment value under pure moment
P	Axial thrust (kips)
P _y =Aσ _y	Axial thrust corresponding to yielding under pure compression
S	Section modulus about the strong axis (in ³)
Z	Plastic modulus about the strong axis (in ³)
b	Flange width
c	Distance from centroid to outer fiber
d	Depth of section
e	Eccentricity (inches)
$k=\sqrt{P/EI}$	
r	Radius of gyration about the strong axis
t	Thickness of flange
w	Thickness of web
x	Distance along the axis of a member, as shown on Fig. 1
y	Deflection (inches)

VIII. Nomenclature (cont'd)

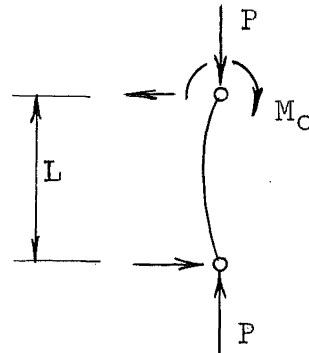
$\frac{ec}{r^2}$	Eccentricity ratio
L/r	Slenderness ratio
$\alpha,$	Non-dimensional constants
$\xi = \frac{\sigma_y}{\pi^2 E}$	Constant defining properties of material
δ	Deflection at specific station along the member (inches)
θ	End rotation (radians)
ϕ	Curvature (radians/inch)
$\phi_y = \frac{2\sigma_y}{Ed}$	Curvature corresponding to initial yield under pure moment
λ	Length of equally spaced segments of total member length
ϵ	Strain (inches/inch)
ϵ_y	Strain corresponding to initial yield point stress
σ	Stress (lbs/inch ²)
σ_y	Yield stress (assumed to be 33 ksi for A7 steel)

TABLE 1

CONSTANTS FOR INTERACTION CURVE EQUATIONS



Loading Condition "c"



Loading Condition "d" *

$$\frac{M_o}{M_p} = 1.0 - K \left(\frac{P}{P_y} \right) - J \left(\frac{P}{P_y} \right)^2$$

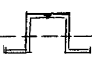
$$\frac{M_o}{M_p} = B - G \left(\frac{P}{P_y} \right)$$

$\frac{L}{r}$	Condition "c"		Condition "d" *	
	K	J	G	B
0	0.42	0.77	1.11	1.13
5	0.49	0.69	1.13	1.14
10	0.56	0.61	1.15	1.14
15	0.63	0.53	1.17	1.14
20	0.70	0.46	1.18	1.14
25	0.77	0.39	1.19	1.14
30	0.85	0.31	1.21	1.15
35	0.92	0.24	1.22	1.15
40	0.99	0.17	1.23	1.16
45	1.08	0.08	1.25	1.16
50	1.17	-0.01	1.27	1.16
55	1.26	-0.10	1.29	1.17
60	1.35	-0.21	1.32	1.17
65	1.45	-0.32	1.36	1.18
70	1.56	-0.44	1.41	1.18
75	1.68	-0.57	1.46	1.19
80	1.81	-0.72	1.52	1.19
85	1.93	-0.88	1.60	1.20
90	2.07	-1.05	1.69	1.21
95	2.22	-1.24	1.79	1.21
100	2.38	-1.45	1.90	1.22
105	2.55	-1.68	2.03	1.23
110	2.74	-1.93	2.18	1.23
115	2.94	-2.20	2.34	1.24
120	3.16	-2.51	2.53	1.25

*Note: For calculated values of $\frac{M_o}{M_p} > 1.0$, use $\frac{M_o}{M_p} = 1.00$

TABLE 2

TEST RESULTS OF MASON, FISHER and WINTER (9)

(1)	(2)	(3)	(4)	(5)	(6)	(7)
Specimen 	Material*	$\left(\frac{L}{r_x}\right)$	$\frac{ec}{r^2}$	P _{ult} (kips)	$\frac{P_{ult}}{P_y}$	$\left(\frac{L}{r_x}\right)$ Adj.
1/4 x 3 - 49	1	49	0.25	122	0.73	55.6
1/4 x 3 - 69	1	69	0.25	110	0.66	78.4
1/4 x 3 - 108	1	108	0.25	75	0.45	122.7
1/4 x 3 - 49	1	49	0.75	89.3	0.53	55.6
1/4 x 3 - 69	1	69	0.75	77.6	0.46	78.4
1/4 x 3 - 108	1	108	0.75	57.2	0.34	122.7
1/4 x 3 - 49	1	49	1.50	65.9	0.39	55.6
1/4 x 3 - 69	1	69	1.50	58.4	0.35	78.4
1/4 x 3 - 108	1	108	1.50	43.2	0.26	122.7
1/4 x 4 - 36	2	36	0.25	171.8	0.80	41.8
1/4 x 4 - 66	2	66	0.25	143.8	0.67	76.6
1/4 x 4 - 110.5	2	110.5	0.25	87.8	0.41	128.2
1/4 x 4 - 36	2	36	0.75	123.2	0.58	41.8
1/4 x 4 - 66	2	66	0.75	100.1	0.47	76.6
1/4 x 4 - 110.5	2	110.5	0.75	66.2	0.31	128.2
1/4 x 4 - 36	2	36	1.50	84.2	0.39	41.8
1/4 x 4 - 66	2	66	1.50	71.0	0.33	76.6
1/4 x 4 - 110.5	2	110.5	~ 1.215	58.1	0.27	128.2
1/2 x 3 - 53	3	53	0.25	214.2	0.74	57.6
1/2 x 3 - 74	3	74	0.25	188.6	0.65	80.5
1/2 x 3 - 117	3	117	0.25	122.3	0.42	127.2
1/2 x 3 - 53	3	53	1.50	117.2	0.41	57.6
1/2 x 3 - 74	3	74	1.50	101.2	0.35	80.5
1/2 x 3 - 117	3	117	1.50	76.1	0.26	127.2

* $\sigma_{y(1)} = 42.5$ ksi, $\sigma_{y(2)} = 44.5$ ksi, $\sigma_{y(3)} = 39.0$ ksi

TABLE 3
TEST RESULTS OF JOHNSTON and CHENEY (10)

(1)	(2)	(3)	(4)	(5)	(6)	(7)	(8)	(9)
Test No.	Member	Material*	e (inches)	$\left(\frac{L}{r_x}\right)$	$(\sigma_o)_{max}$ (ksi)	$\frac{ec}{r^2}$ (Approx.)	$\frac{P}{P_y}$	$\left(\frac{L}{r_x}\right)_{Adj.}$
C-49	3I5.7	1	1.01	22.6	23.50	1.0	0.56	25.5
C-50	3I5.7	1	1.01	32.6	22.85	1.0	0.54	36.8
C-51	3I5.7	2	1.01	42.1	20.45	1.0	0.50	46.8
C-52	3I5.7	2	1.01	47.1	19.10	1.0	0.47	52.4
C-53	3I5.7	2	1.01	52.1	20.00	1.0	0.49	58.0
C-54	3I5.7	2	1.01	62.0	18.70	1.0	0.46	68.9
C-55	3I5.7	2	1.01	72.0	16.50	1.0	0.40	80.0
C-56	3I5.7	2	1.01	82.0	14.95	1.0	0.37	91.2
C-57	3I5.7	2	1.01	101.8	11.40	1.0	0.28	113.1
C-58	3I5.7	2	1.01	121.6	9.50	1.0	0.23	135.1
C-59	3I5.7	2	0.50	22.3	28.90	0.5	0.71	24.8
C-60	3I5.7	2	1.52	22.3	19.00	1.5	0.47	24.8
C-61	3I5.7	2	2.02	22.3	15.62	2.0	0.38	24.8
C-62	3I5.7	2	3.03	22.3	11.86	3.0	0.29	24.8
C-63	3I5.7	2	5.05	22.3	8.45	5.0	0.21	24.8
C-64	3I5.7	2	7.07	22.3	6.29	7.0	0.15	24.8
C-65	3I5.7	2	0.50	47.1	27.20	0.5	0.67	52.4
C-66	3I5.7	2	1.52	47.1	16.38	1.5	0.40	52.4
C-67	3I5.7	2	2.02	47.1	13.30	2.0	0.33	52.4
C-68	3I5.7	2	3.03	47.1	11.10	3.0	0.27	52.4
C-69	3I5.7	2	5.05	47.1	7.41	5.0	0.18	52.4
C-70	3I5.7	2	7.07	47.1	5.64	7.0	0.14	52.4
C-71	3I5.7	2	0.50	72.0	21.05	0.5	0.52	80.0
C-72	3I5.7	2	1.52	72.0	13.93	1.5	0.34	80.0
C-73	3I5.7	2	2.02	72.0	12.67	2.0	0.31	80.0
C-74	3I5.7	2	3.03	72.0	9.02	3.0	0.22	80.0
C-75	3I5.7	2	5.05	72.0	6.53	5.0	0.16	80.0
C-76	3I5.7	2	7.07	72.0	4.81	7.0	0.12	80.0
6-5	6WF20	3	2.23	46.7	21.6	1.0	0.54	51.2
6-6	6WF20	3	4.45	46.9	14.4	2.0	0.36	51.4

* $\sigma_y(1) = 42.2$ ksi, $\sigma_y(2) = 40.8$ ksi, $\sigma_y(3) = 39.8$ ksi

TABLE 4
TEST RESULTS of MASSONNET (12)

(1)	(2)	(3)	(4)	(5)	(6)	(7)	(8)	(9)
Test No.	Section	Loading Condition	$\frac{ec}{r^2}$	P_{max} (tons)	P_y (tons)	$\left(\frac{L}{r_x}\right)$	$\frac{P}{P_y}$	$\left(\frac{L}{r_x}\right)$ Adj.
1	DIE 20	c	0.5	88.8	132	23.6	0.67	24.1
2	DIE 20	c	1.0	66.8	132	23.7	0.51	24.2
3	DIE 20	c	3.0	35.8	132	23.7	0.27	24.2
8	DIE 20	c	0.5	84.8	134	35.6	0.63	36.3
9	DIE 20	c	1.0	64.8	133	35.4	0.49	36.1
10	DIE 20	c	3.0	32.8	133	35.5	0.25	36.2
16	DIE 20	c	0.5	71.0	135	44.4	0.53	45.3
17	DIE 20	c	1.0	59.0	134	44.2	0.44	45.1
18	DIE 20	c	3.0	32.5	134	44.4	0.24	45.3
24	DIE 20	c	0.5	62.0	134	59.1	0.46	60.4
25	DIE 20	c	1.0	53.5	133	58.7	0.40	60.0
26	DIE 20	c	3.0	29.0	134	59.2	0.22	60.4
33	DIE 10	c	0.5	22.8	53.8	80.8	0.42	87.0
34	DIE 10	c	1.0	19.3	54.5	82.4	0.35	88.6
35	DIE 10	c	3.0	11.5	55.0	82.6	0.21	89.1
42	DIE 10	c	0.5	13.8	57.1	109.9	0.24	118.2
43	DIE 10	c	1.0	12.4	55.6	110.3	0.22	119.0
44	DIE 10	c	3.0	9.05	55.7	109.6	0.16	118.0
4	DIE 20	d	0.5	95.0	133	23.6	0.72	24.1
5	DIE 20	d	1.0	78.8	133	23.6	0.59	24.2
11	DIE 20	d	0.5	93.8	134	35.6	0.70	36.3
12	DIE 20	d	1.0	74.8	133	35.3	0.56	36.1
13	DIE 20	d	3.0	40.3	133	35.2	0.30	36.0
19	DIE 20	d	0.5	90.8	133	47.4	0.68	48.1
20	DIE 20	d	1.0	70.0	133	47.7	0.53	48.4
21	DIE 20	d	3.0	39.0	134	47.7	0.29	48.4
27	DIE 20	d	0.5	82.0	133	59.0	0.62	60.2
28	DIE 20	d	1.0	67.0	135	59.6	0.50	60.8
29	DIE 20	d	3.0	38.1	135	59.2	0.28	60.4
36	DIE 10	d	0.5	25.0	56.4	81.9	0.44	88.2
37	DIE 10	d	1.0	24.4	56.4	82.7	0.43	89.2
38	DIE 10	d	3.0	15.05	57.0	82.7	0.26	89.2
45	DIE 10	d	0.5	11.8	57.7	109.1	0.20	117.8
47	DIE 10	d	3.0	10.8	57.7	109.1	0.19	117.8

TABLE 5

TEST RESULTS of WISCONSIN SERIES (13)

(1)	(2)	(3)	(4)	(5)	(6)	(7)	(8)
Test No.	Member	$\frac{ec}{r^2}$	$\left(\frac{L}{r_x}\right)$	σ_{ult} (ksi)	σ_y (ksi)	$\frac{P}{P_y}$	$\left(\frac{L}{r_x}\right)$ Adj.
H-1	8H32	1.00	11.4	20.7	37.4	0.55	12.1
H-2	8H32	1.00	29.0	19.95	37.4	0.53	30.9
H-3	8H32	1.00	49.5	17.95	37.4	0.48	52.7
H-4	8H32	1.00	69.6	15.10	38.0	0.40	74.6
H-5	8H32	1.00	89.7	12.60	36.4	0.35	94.2

TABLE 6

TEST RESULTS OF THE CURRENT LEHIGH TEST SERIES

(1)	(2)	(3)	(4)	(5)	(6)	(7)	(8)
Test No.	Member	Loading Condition	Experimental*				$\left(\frac{L}{r_x}\right)$ Adj.
			$\sigma_y = 40 \text{ ksi}^+$		Adjusted $\sigma_y^\#$		
			P/P _y	M _o /M _p	P/P _y	M _o /M _p	
T-8	8WF31	c	0.62	<u>0.12</u>	0.68	<u>0.13</u>	58
T-11	8WF31	c	0.87	<u>0</u>	0.95	<u>0</u>	58
T-12	8WF31	c	<u>0.12</u>	0.84	<u>0.13</u>	0.92	58
T-15	8WF31	c	<u>0.85</u>	<u>0</u>	0.93	<u>0</u>	43
T-16	8WF31	c	<u>0.12</u>	0.78	<u>0.13</u>	0.85	43
T-18	8WF31	c	0.91	<u>0</u>	0.99	<u>0</u>	28
T-19	8WF31	c	<u>0.12</u>	0.81	<u>0.13</u>	0.88	28
T-20	4WF13	c	<u>0.12</u>	0.84	<u>0.12</u>	0.87	60
T-26	4WF13	c	<u>0.12</u>	0.79	<u>0.12</u>	0.81	91
T-28	4WF13	c	0.80	<u>0</u>	0.82	<u>0</u>	91
T-32	4WF13	c	<u>0.12</u>	0.76	<u>0.12</u>	0.78	120
T-13	8WF31	d	<u>0.12</u>	1.05	<u>0.13</u>	1.14	58
T-23	4WF13	d	<u>0.12</u>	1.05	<u>0.12</u>	1.08	91
T-31	4WF13	d	<u>0.12</u>	0.98	<u>0.12</u>	1.01	120

* Parameters that were held constant are underlined.

+ $\sigma_y = 40 \text{ ksi}$ determined from tension coupon tests.

Adjusted σ_y (to take into account the influence of strain rate) was obtained by pro-rating the tension coupon value in the same ratios as those given in Ref. 15. (Note: values change for different sections.)

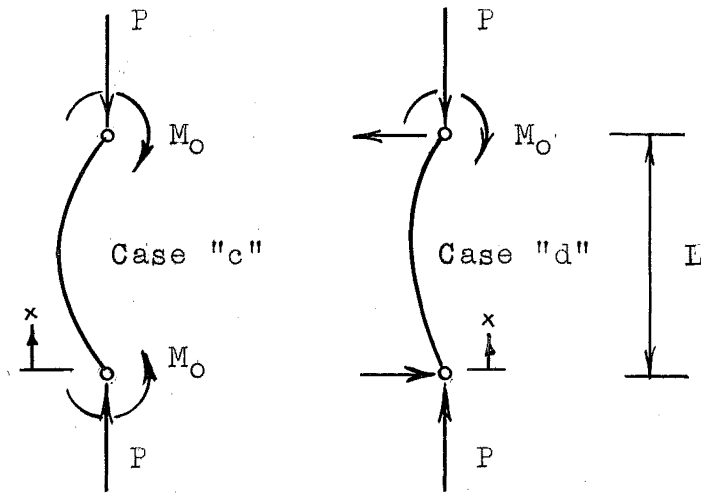


Fig. 1 CONDITIONS OF LOADING

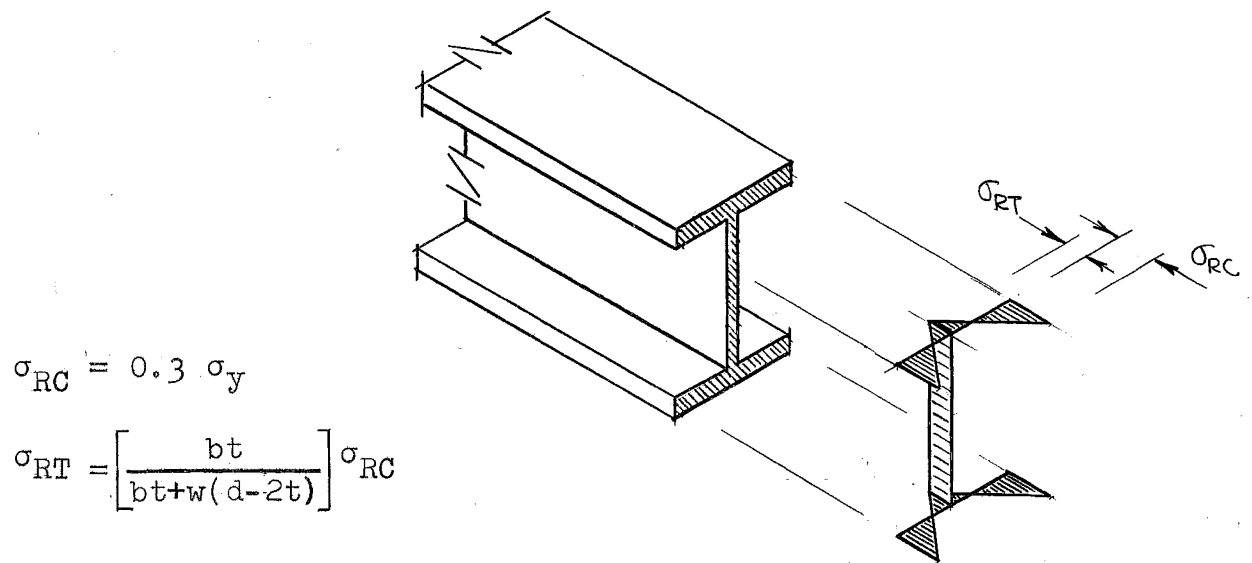


Fig. 2 ASSUMED COOLING RESIDUAL STRESS' PATTERN

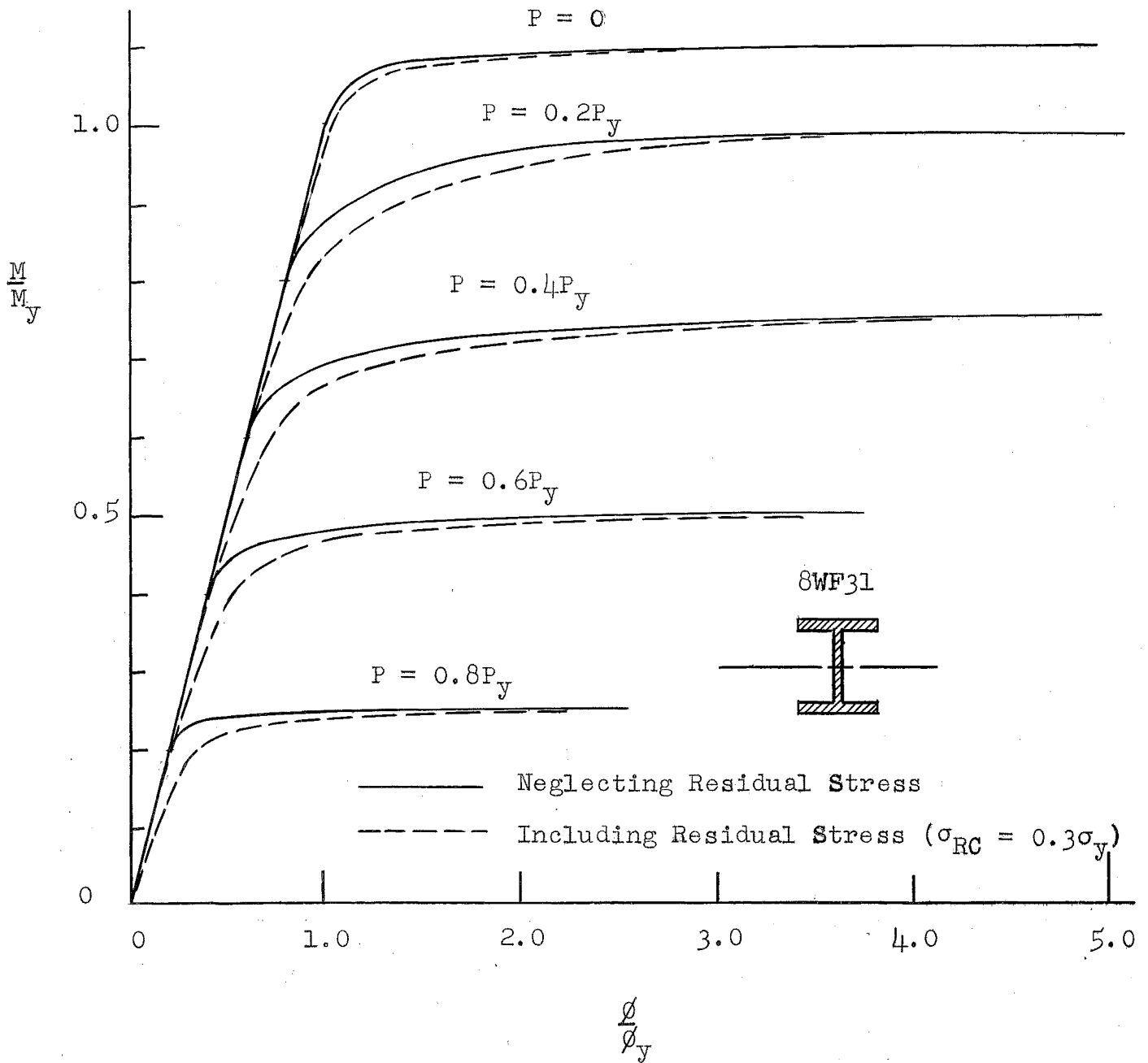


Fig. 3 MOMENT-THRUST-CURVATURE RELATIONSHIP FOR AN 8WF31 SECTION, INCLUDING THE INFLUENCE OF RESIDUAL STRESS(2)

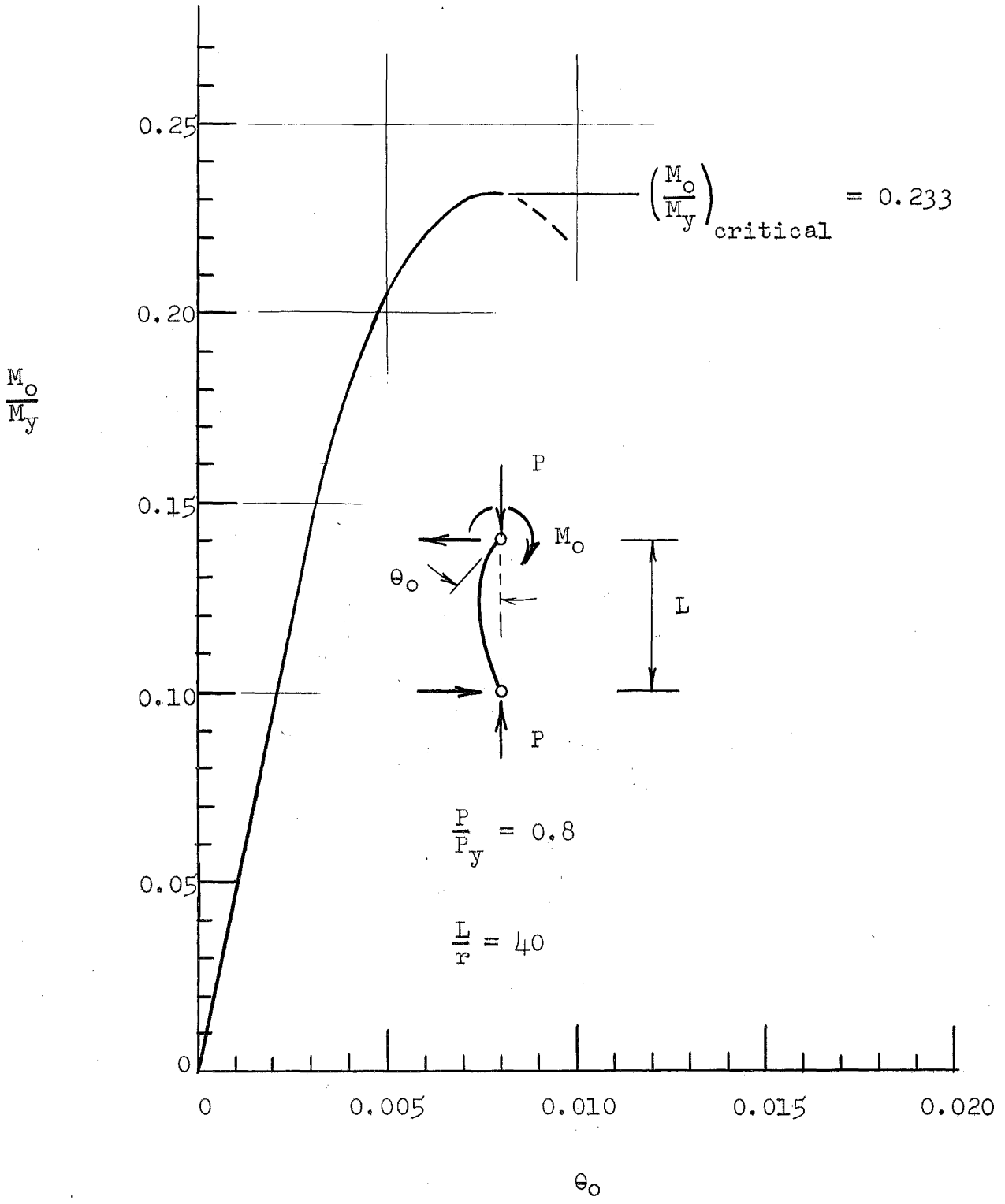
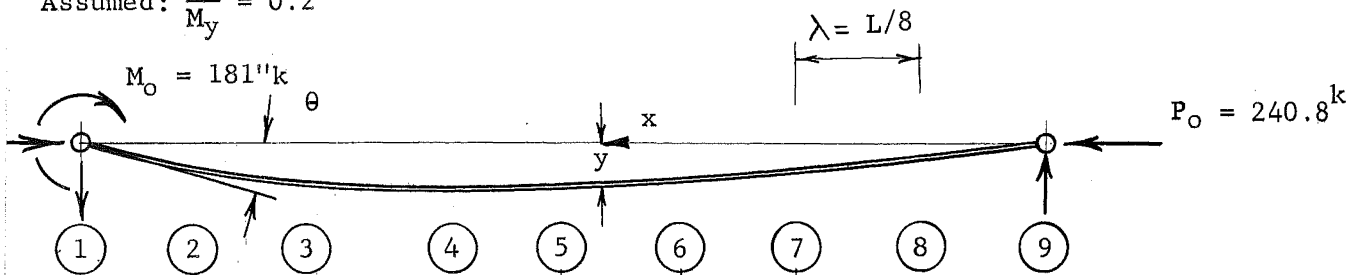


Fig. 4 TYPICAL MOMENT VERSUS END ROTATION CURVE FOR CONDITION "a" LOADING

Given: $\frac{L}{r_x} = 40$; $\frac{P_o}{P_y} = 0.8$; 8WF31 Section; $L = 138.8''$; $\lambda = 17.35''$

Assumed: $\frac{M_o}{M_y} = 0.2$



First Trial									MF*	Notation
181	158	136	113	90	68	45	23	0		Moment due to M_o
0	0.026	0.049	0.068	0.047	0.044	0.032	0.008	0		Assumed Deflection
0	5	10	14	10	9	7	2	0		Moment due to P_o
181	163	146	127	100	77	52	25	0		Total Moment (a + c)
0.200	0.180	0.161	0.140	0.111	0.085	0.058	0.028	0		M_x/M_y
0.350	0.290	0.250	0.210	0.151	0.119	0.083	0.045	0	$\lambda\phi_y$	Concentrated Angle Changes **
	0.350	0.640	0.890	1.100	1.251	1.370	1.453	1.498	$\lambda\phi_y$	Slope
0	0.350	0.990	1.880	2.980	4.231	5.601	7.045	8.552	$\lambda^2\phi_y$	Deflection Correction
0	1.069	2.138	3.207	4.276	5.345	6.141	7.483	8.552	$\lambda^2\phi_y$	to Deflection
0	0.719	1.143	1.327	1.296	1.114	0.540	0.429	0	$\lambda^2\phi_y$	Final Deflection
0	0.060	0.095	0.110	0.107	0.092	0.045	0.036	0		Final Deflection in Inches

Fourth Trial									Assumed
0	0.069	0.112	0.131	0.129	0.112	0.081	0.043	0	Deflection***
0	0.070	0.113	0.132	0.130	0.112	0.082	0.043	0	Final Deflection

* Multiplication Factor

** From Fig. 3, corresponding to $\frac{M_x}{M_y}$

*** Line k from third trial = line a' of fourth trial

The corresponding endslope $\theta = \frac{4 \times 0.070 - 0.113}{2 \times 17.35} = 0.00481$

Fig. 5 TYPICAL NUMERICAL INTEGRATION PROCEDURE TO OBTAIN END SLOPE

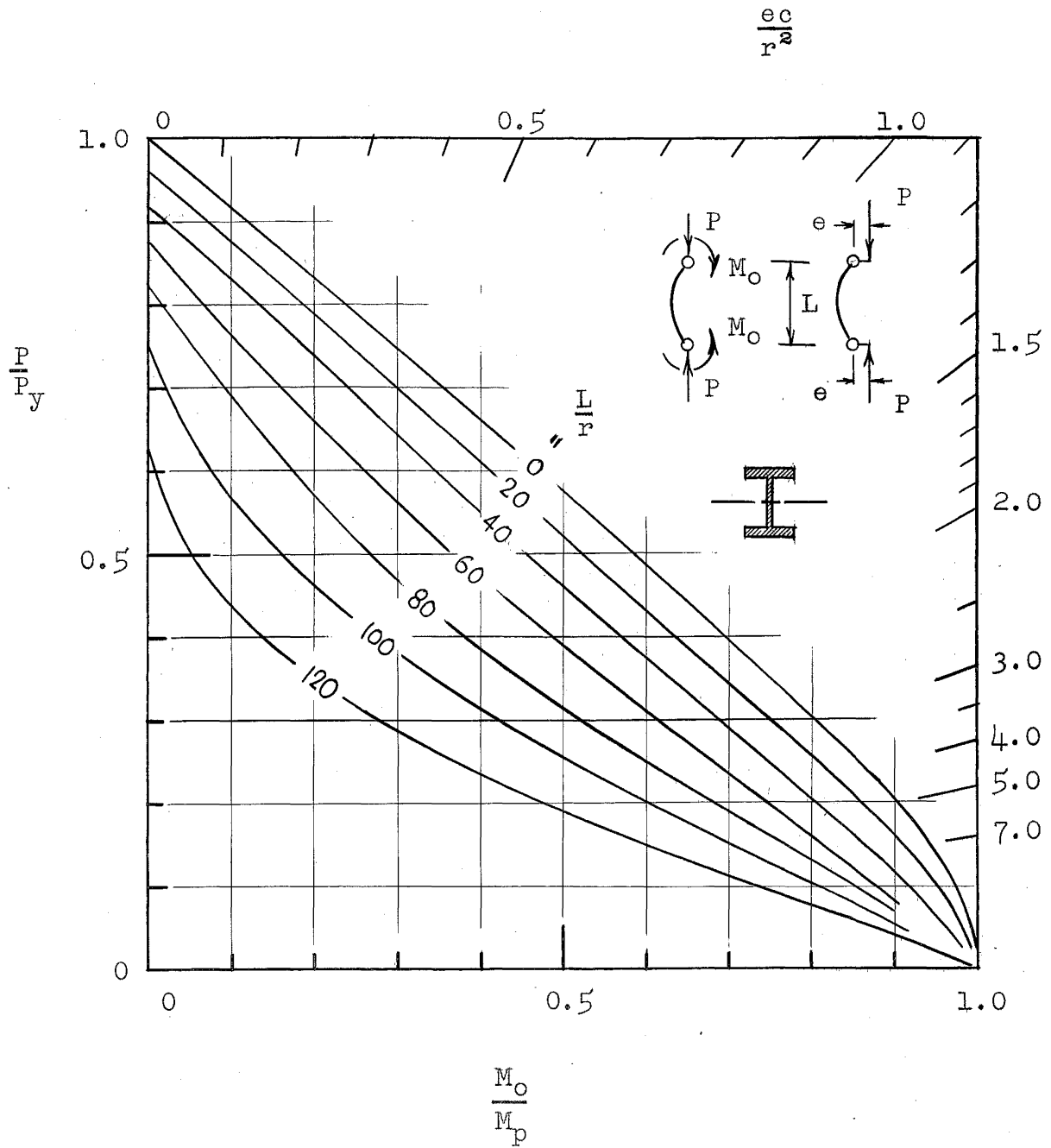


Fig. 6 MAXIMUM CARRYING CAPACITY INTERACTION CURVES FOR CONDITION "c" LOADING (INCLUDING THE INFLUENCE OF RESIDUAL STRESS)

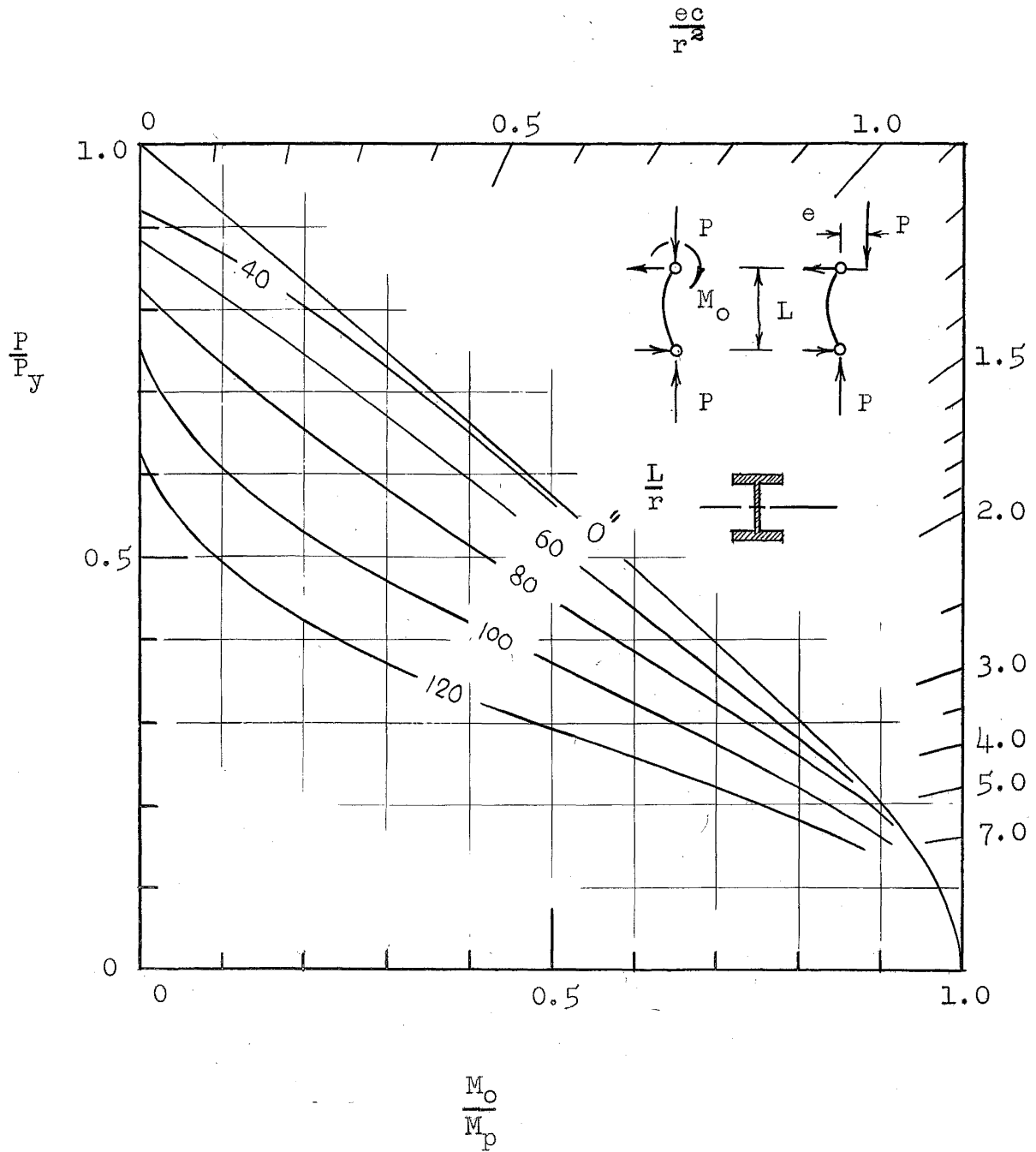


Fig. 7 MAXIMUM CARRYING CAPACITY INTERACTION CURVES FOR CONDITION "d" LOADING (INCLUDING THE INFLUENCE OF RESIDUAL STRESS)

———— Neglecting Influence of Residual Stress
 - - - - - Including Influence of Residual Stress

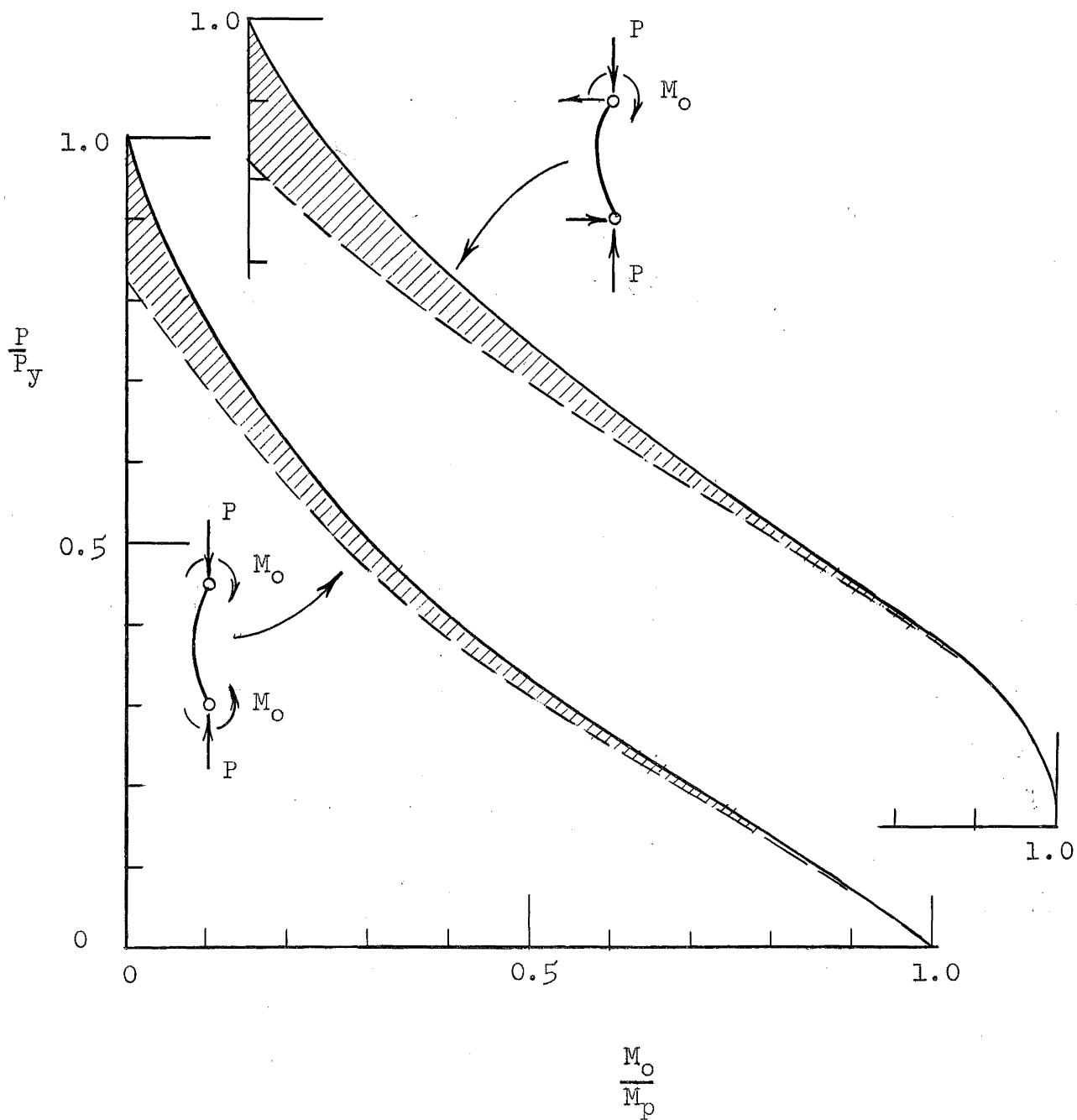


Fig. 8 INTERACTION CURVES FOR $\frac{L}{r} = 80$ SHOWING INFLUENCE OF RESIDUAL STRESS

205A.21

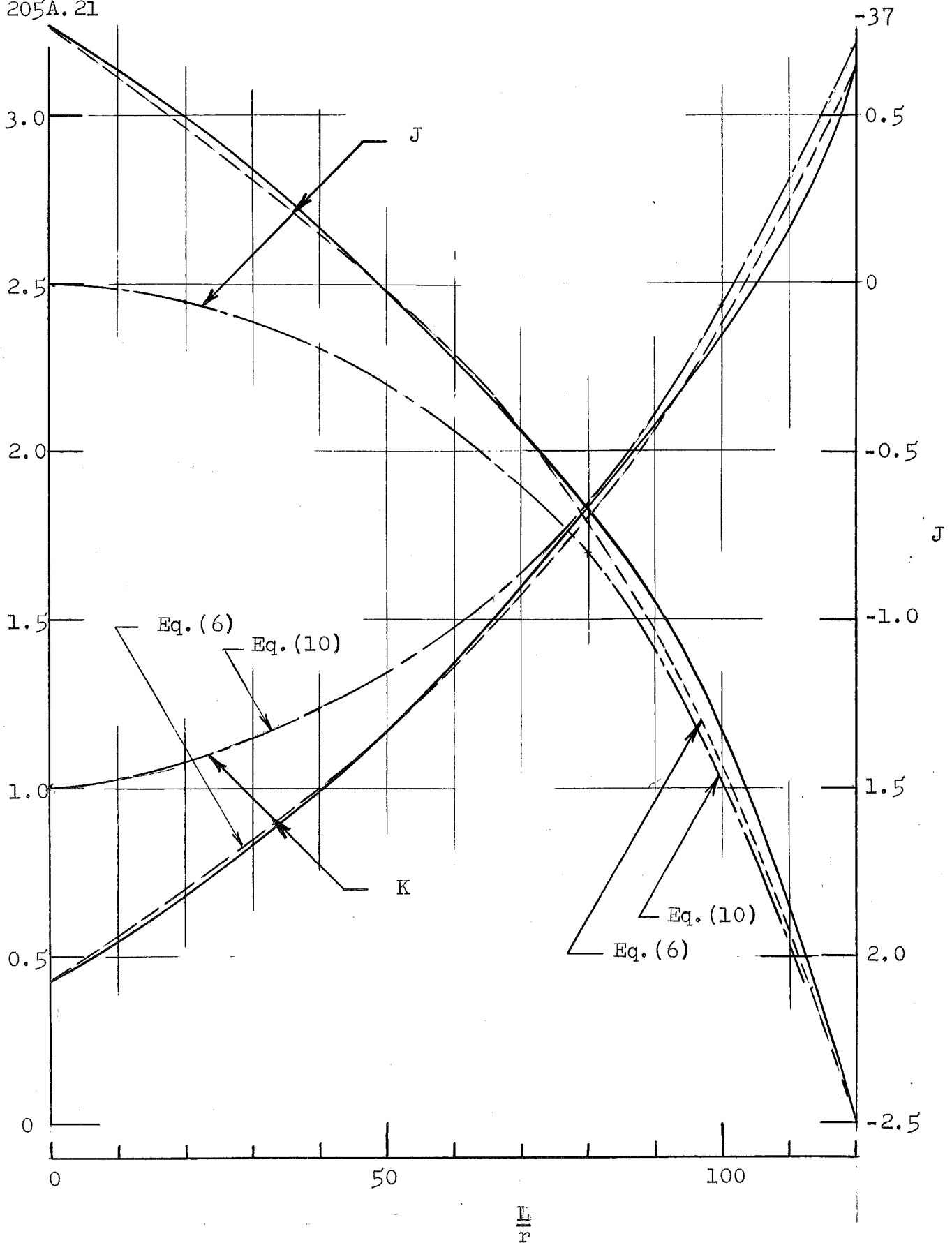


Fig. 9 COEFFICIENTS FOR LOADING CONDITION "c"
INTERACTION EQUATION

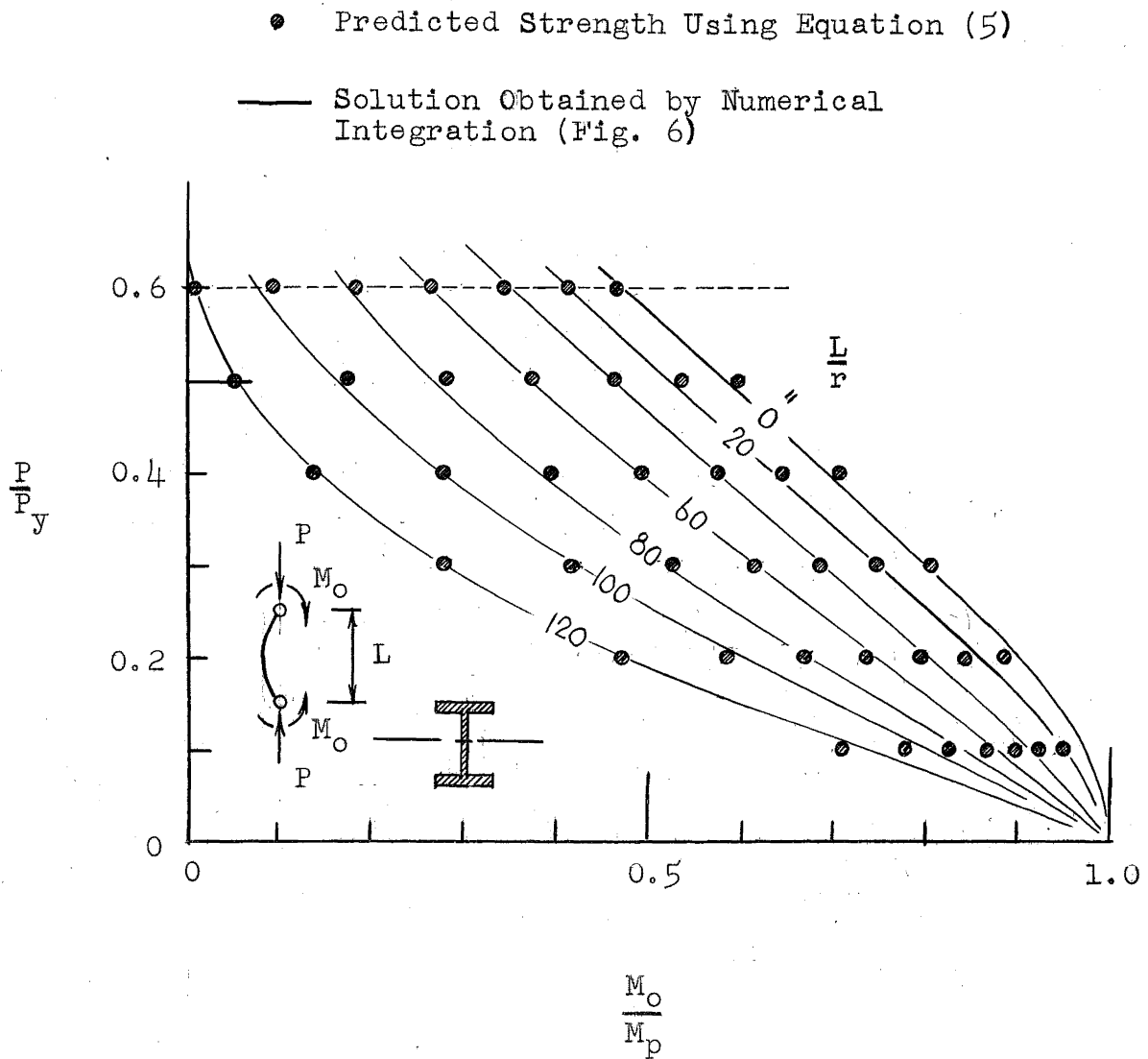


Fig. 10 COMPARISON BETWEEN "EXACT" AND "APPROXIMATE" INTERACTION CURVES (LOADING CONDITION "c")

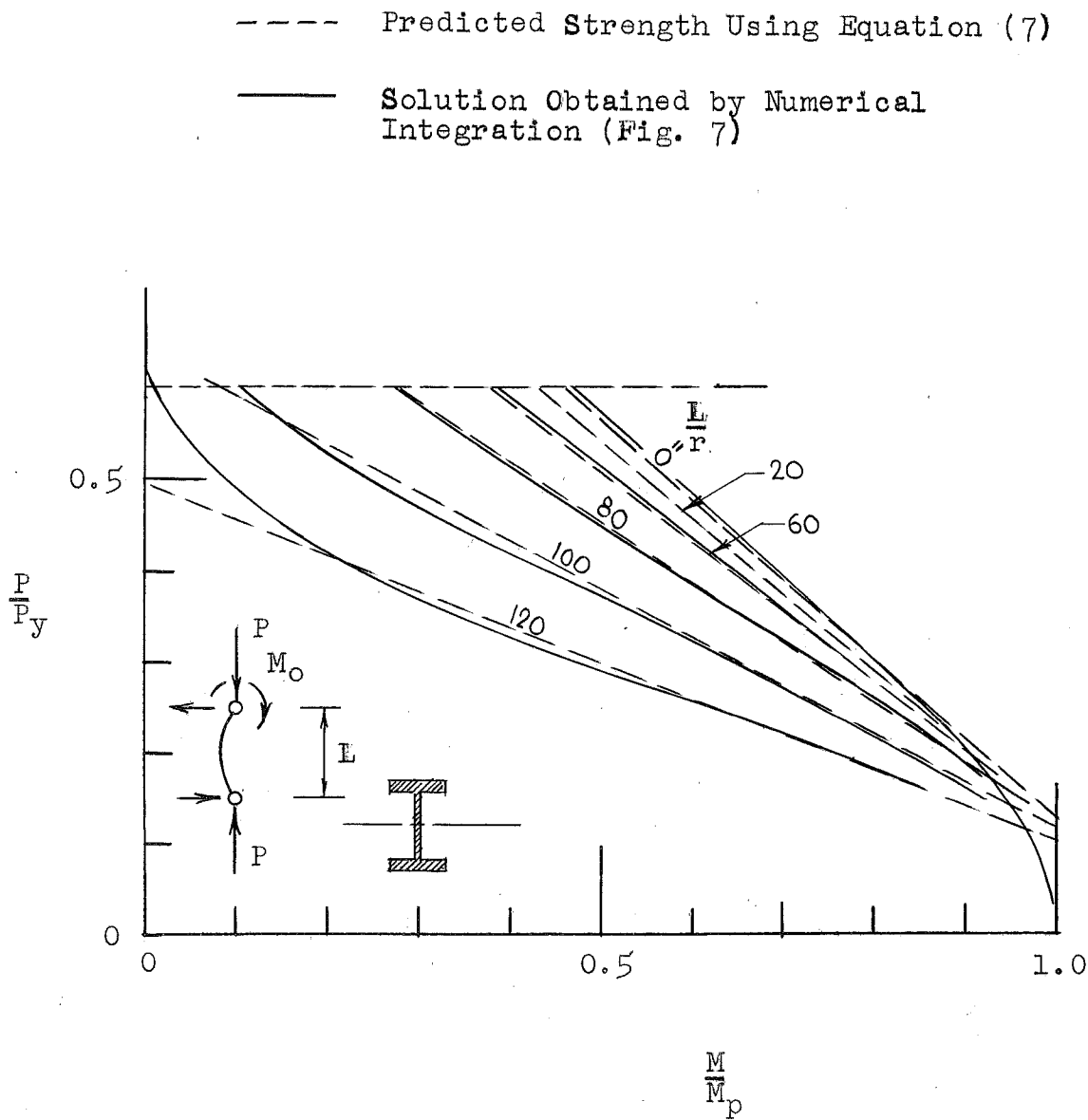


Fig. 11 COMPARISON BETWEEN "EXACT" AND "APPROXIMATE" INTERACTION CURVES (LOADING CONDITION "d")

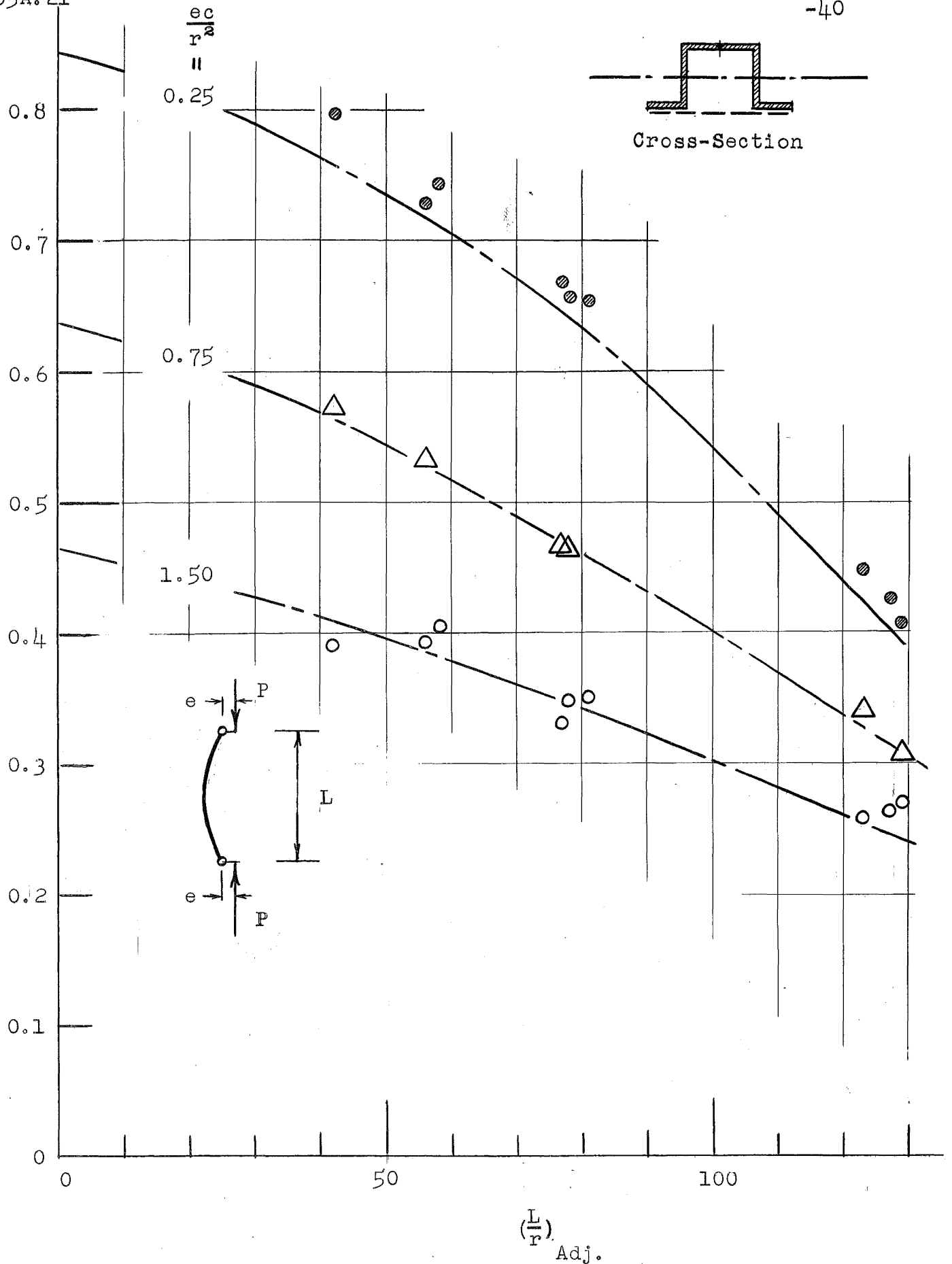


Fig. 12 COMPARISON OF COLUMN TEST RESULTS BY MASON, FISHER AND WINTER (9) WITH PREDICTED STRENGTHS

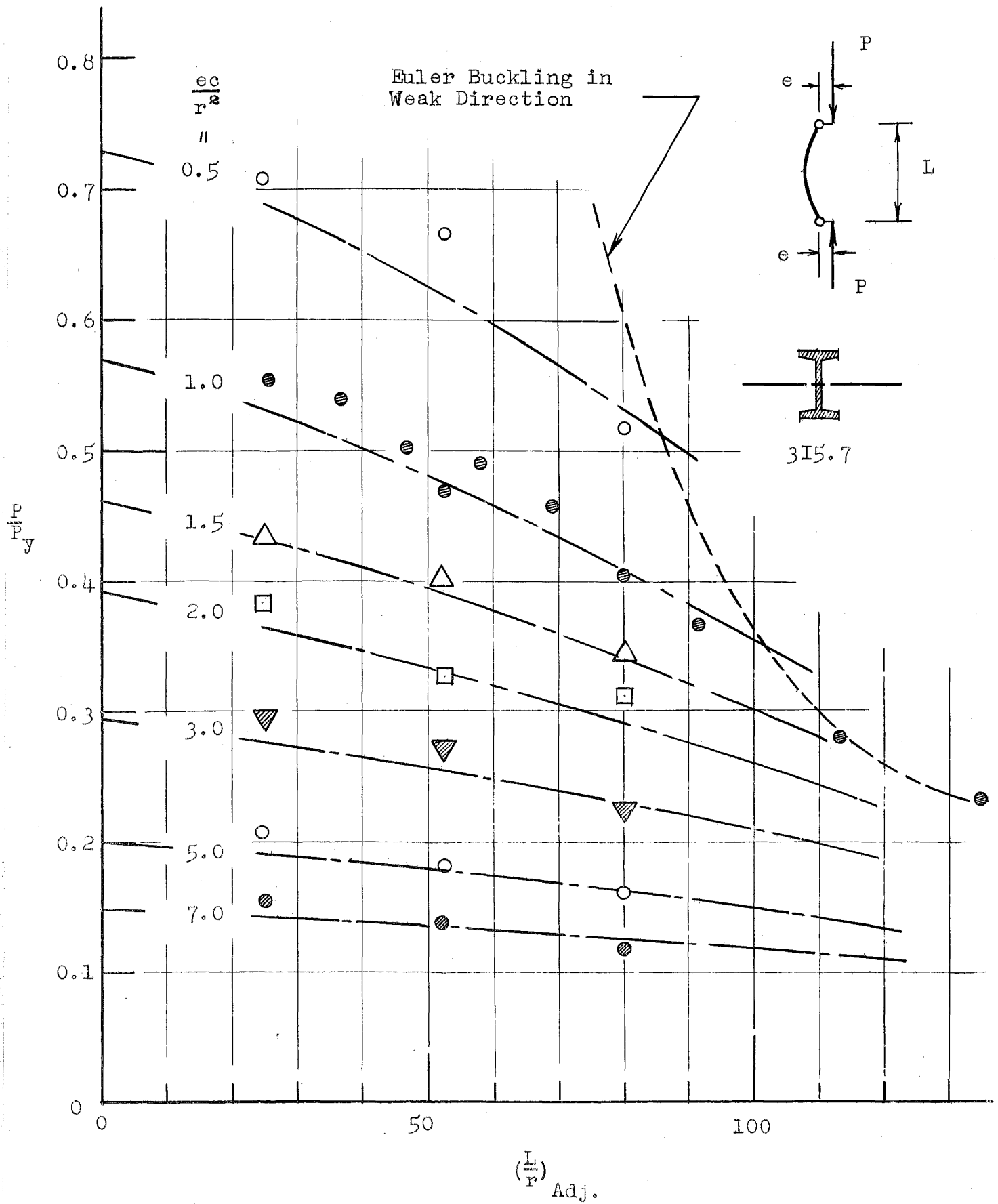


Fig. 13 COMPARISON OF COLUMN TEST RESULTS BY JOHNSTON AND CHENEY⁽¹⁰⁾ WITH PREDICTED STRENGTHS

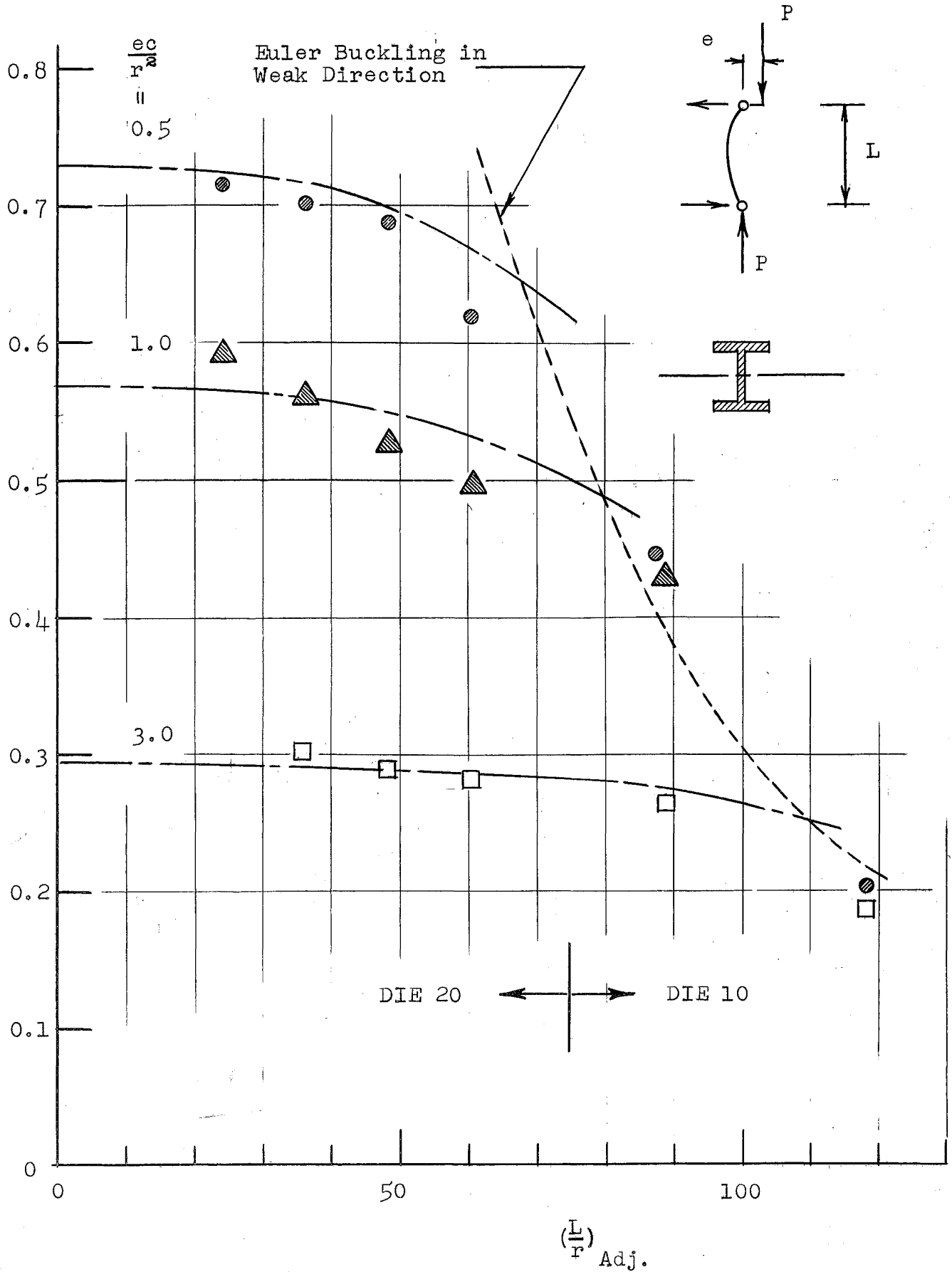


Fig. 14 COMPARISON OF COLUMN TEST RESULTS BY MASSONNET⁽¹²⁾ WITH PREDICTED STRENGTHS

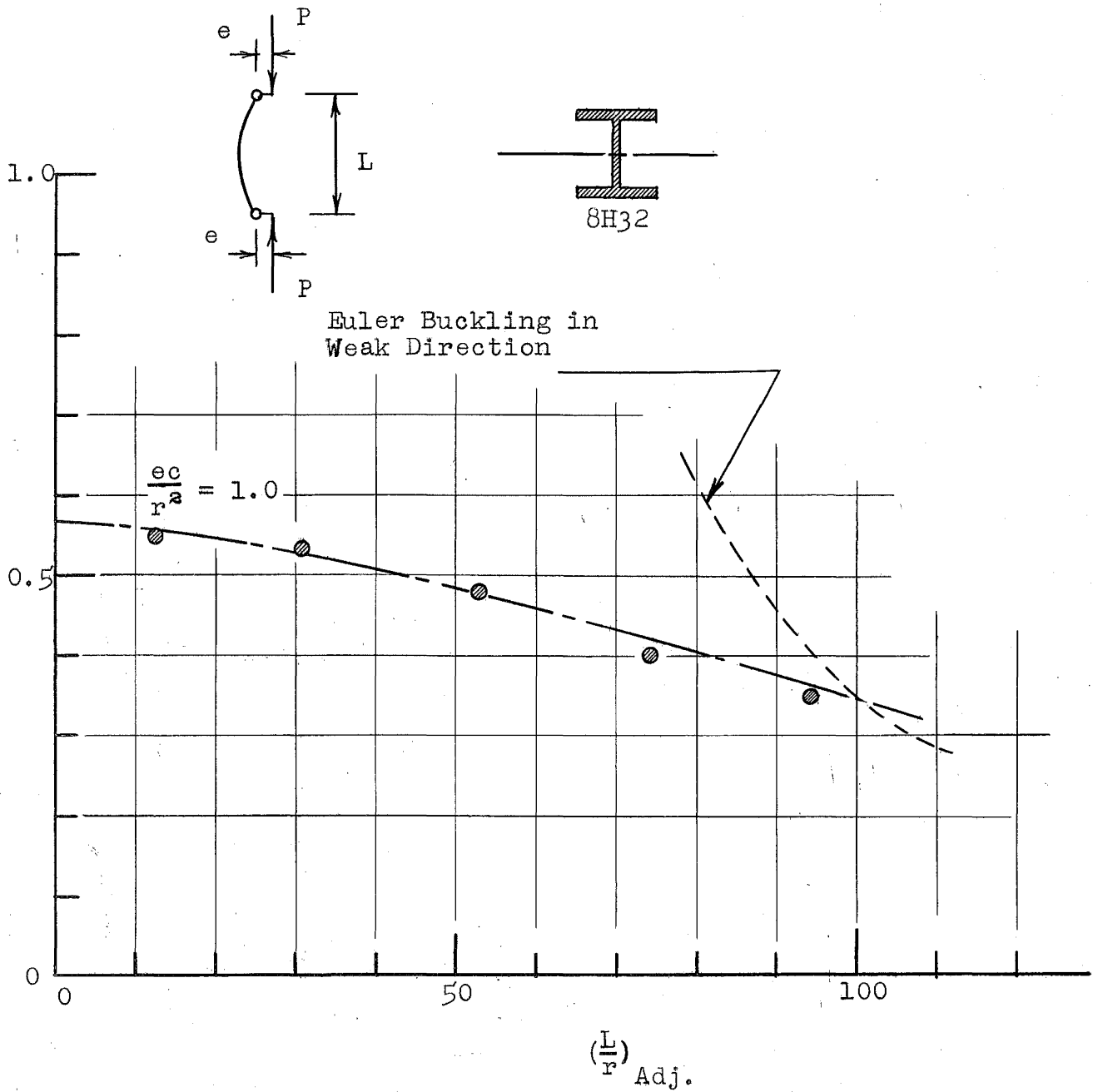


Fig. 15 COMPARISON OF WISCONSIN COLUMN TEST RESULTS⁽¹³⁾ WITH PREDICTED STRENGTHS

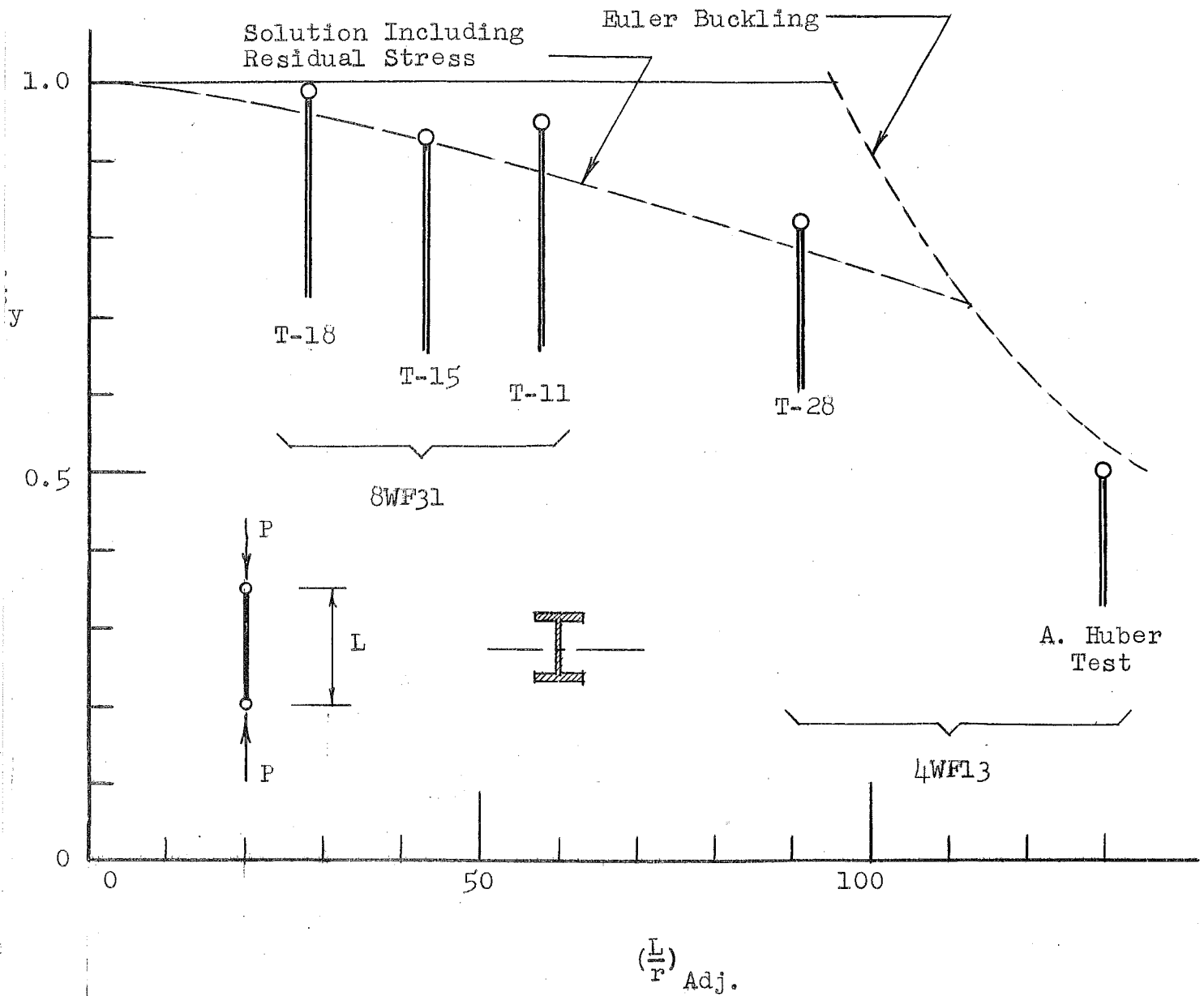


Fig. 16 COMPARISON OF CURRENT LEHIGH SERIES OF TESTS WITH PREDICTED STRENGTHS